Predicting Thermal Contact Resistance in Circuit Card Assemblies

Scott H. Kunkel and Wiley M. Peck

E-Systems, Melpar Division
7700 Arlington Boulevard
Falls Church, VA 22046

Abstract

On a typical conduction-cooled Circuit Card Assembly (CCA) there is a temperature rise caused by the resistance between component die, Printed Circuit Board (PCB), thermal frame (heat sink), and chassis. While the resistance at the component junction, through the PCB, and through the thermal frame can be readily calculated from material properties, modeling the thermal frame and card clamp to chassis interface can be difficult. For CCA power below approximately 25 watts the loss at the interface is usually less than 4°C (0.30°C/W for bare aluminum). As the thermal dissipation on a CCA reaches 50-75 watts (>1 watt/in^2 on VME 1101.2 format), it becomes necessary to model this interface because of its increasing influence on the overall temperature rise. A method utilizing several Unigraphics® GRIP® routines, SINDA® thermal analysis software, and empirical data has been developed that predicts the thermal interface performance between both the chassis and thermal frame, and the chassis and card clamp to within 30 percent of measured values.

Introduction

The majority of military airborne electronics presently being developed use conduction cooling for thermal management. Conduction cooling at the CCA level provides a lightweight, high reliability, low maintainability system as compared to forced-air convection, especially at high altitudes. When utilizing conduction cooling, the rise in temperature due to the thermal path shown in Figure 1 must be estimated in order to provide reliable designs. Many recent material advances, such as carbon composites, have greatly reduced the thermal rise associated with the thermal frame. These advances have allowed designers to implement CCA designs in the 50-75 watt range.[1] With increased power dissipation, the interface between the thermal frame and chassis becomes a more significant factor in the overall management of thermal resistance. A computer model of this interface will allow a designer to evaluate the changing effects of the controllable parameters.

The two parameters of interest in creating a computer model of the interface (Figure 2) are the heat sink material characteristics and the card clamp characteristics. The material characteristics are divided into material properties and machining characteristics. The material properties that influence contact resistance are conductivity, hardness, and stiffness. The machining characteristics related to the material surface condition include the surface finish, flatness or waviness, and the angle or slope of the average asperity (Figure 2). The card clamp characteristics for wedge clamps include wedge angle versus pressure, number of pieces in the clamp, load distribution along the clamp, contact area, pressure, and coefficient of friction.

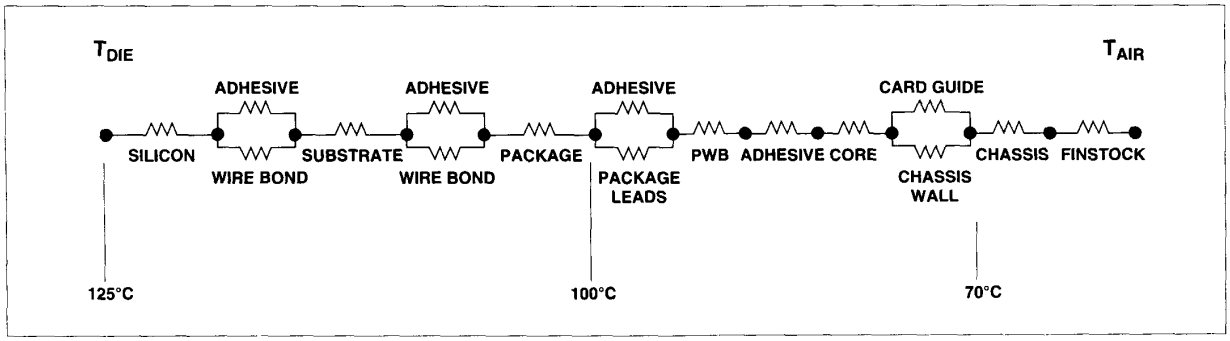

Figure 1. Thermal Resistance Path

Heat Sink Material Characteristics

Figure 3 shows how each heat sink material parameter (listed below the Y-axis) affects the overall contact resistance. Each

Unigraphics® and GRIP® are registered trademarks of Electronics Data Systems Corporation.
SINDA® is a registered trademark of the National Aeronautics and Space Administration.

0-7803-1372-0/$3.00

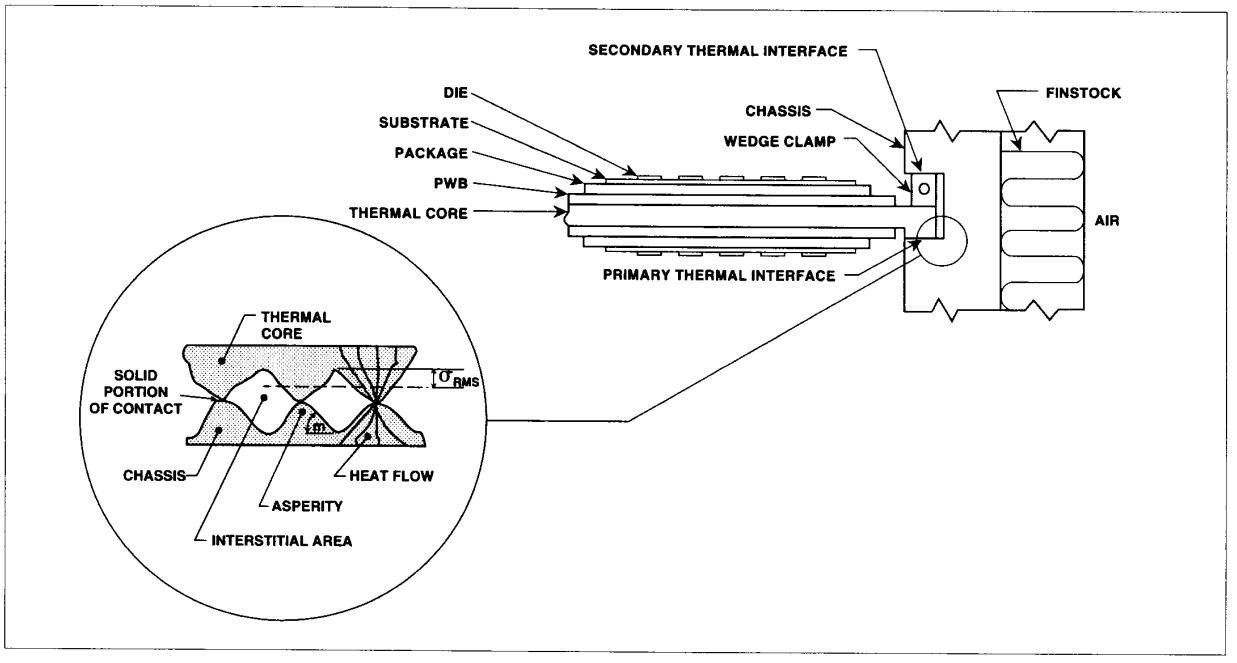

Figure 2. Thermal Interface

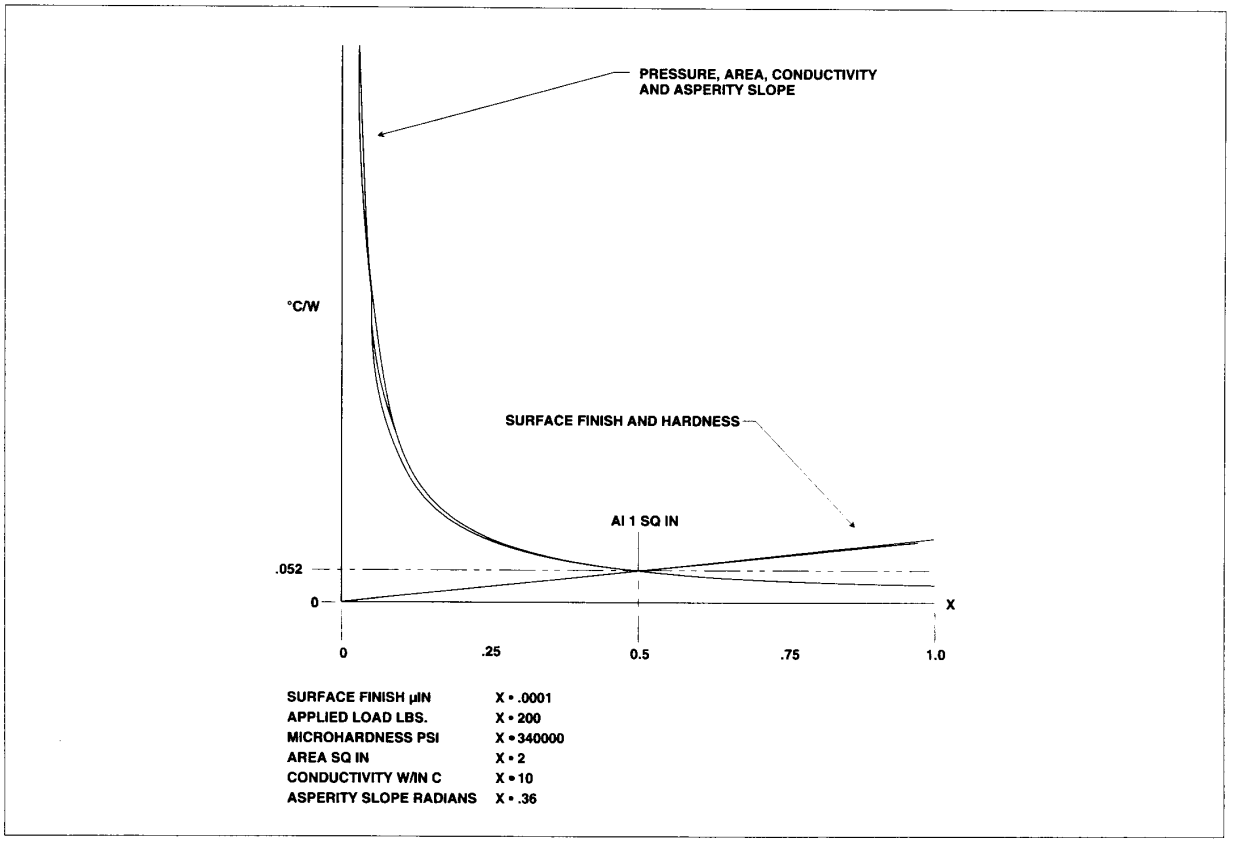

Figure 3. Contact Resistance Versus Material/Clamping Characteristics

curve represents five of the six parameters held constant, while the sixth is allowed to vary (see eq.(2)). The intersection point of all the curves represents 6061-T6 aluminum with the following characteristics: surface finish of 50 micro-inches, asperity slope of 0.18 radian, microhardness of 170,000 psi, area of 1 in^2, conductivity of 5 W/in.°C, and an applied load of 100 lbs.

The figure shows that no single parameter dominates the equation. Small changes in the lower ranges (<0.25) of pressure, area, conductivity, and asperity slope can have a significant effect on the resistance, whereas the surface finish and material hardness follow a relatively linear curve. The figure also shows that, at the upper extremes (>0.75), the surface finish and hardness have a larger impact on the overall resistance than the four previously mentioned parameters.

Card Clamp Characteristics

A wedge style card clamp, shown in Figure 4, is frequently used to secure CCAs in current airborne chassis designs. Several companies manufacture wedge clamps in either end-fixed or center-fixed configurations and with various numbers of wedges. In an end-fixed configuration, when the clamp is compressed, all the wedges translate downward toward the last wedge, which is fixed in relation to all other wedges. In the center-fixed configuration, the center wedge is fixed to the CCA and the wedges on either end of the clamp are pulled toward it. The computer model and associated data show that the center fixed clamp with five or more wedges provides better heat transfer than a comparable end-fixed clamp. This is due to lower friction losses and a better load distribution in the center-fixed configuration, which helps transfer heat through the primary thermal interface; and to an increased interface area between clamp wedges, which improves the transfer through the secondary thermal interface (Figure 2).

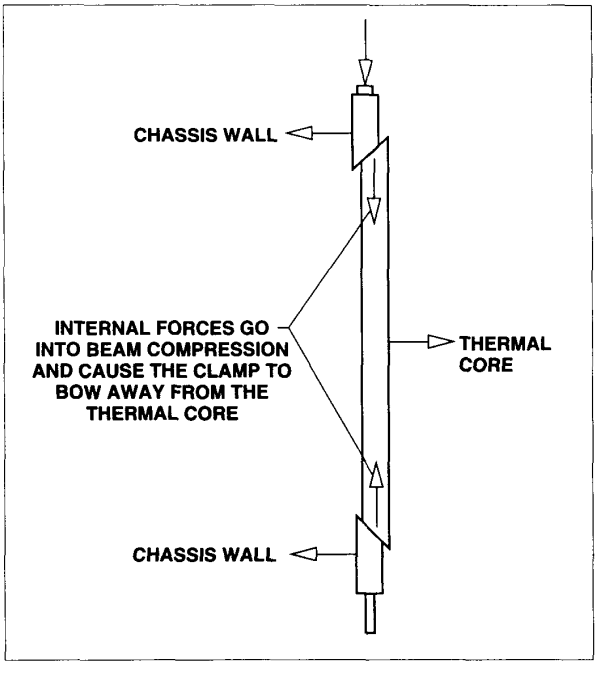

Figure 4. Three-piece Wedge Clamp

Modeling the Interface

Typical wedge clamps utilize a 45-degree angle wedge for ease of manufacture, which minimizes overall clamp vertical travel (parallel to CCA) and maintains a relatively large horizontal expansion range. This design also allows each piece to decouple from its adjacent piece when the pressure is released. Figure 5 shows the calculated values of wedge angle versus side wall force for a range of coefficients of friction. The figure indicates that the side wall force is higher for smaller wedge angles, but this advantage is offset by an increased possibility for galling that reduces the clamp's ability to decouple, decreased horizontal range for expansion, and increased verticle travel.

An additional observation is that the total side wall force seems to increase with the number of wedges in a given clamp. Figure 6 shows that the force approaches a value of 382 pounds asymptotically for a given coefficient of friction (0.35) and given input force, and that the delta increase in force seems to become insignificant after approximately nine pieces for this scenario. Assuming that the total energy imparted in any clamp, regardless of the number of pieces, is approximately the same for a given input torque, then the perceived delta difference in force comes from the actual energy that goes into compressing the center piece. In the three-piece clamp more force goes into compressing the center piece; in the five- or seven-piece clamp, the compressive force goes into expanding another set of wedges. This provides better distribution of the total clamping force over the thermal interface and improves heat transfer.

Figure 7 shows how the forces exerted by each individual piece in a given clamp are distributed. The results from these examples are based on specific input data; ie., coefficient of friction of .3, surface finish of 85 micro-inches, microhardness of 170,322 psi, and a resultant applied load (from the screw torque) of 267 lbs. The force is not uniformly distributed among the pieces. This is due to friction losses along the clamp to the chassis wall, and between the wedge pieces themselves. If the coefficient of friction is relatively low, the maximum variance between the top wedge and the last wedge will be insignificant. (Note that this applies to end-fixed clamps from top to bottom, and to center-fixed clamps from either top or bottom to the clamp center piece.) If the coefficient of friction is relatively high (which for bare aluminum is quite common), the applied load may not theoretically reach the last wedge. Figure 7 shows the free body diagram of a center-fixed and an end-fixed five-piece clamp. The friction angle is determined by using eq.(1), and basic force summations are used to calculate the reaction forces. These reaction forces are either a sidewall force or the adjacent wedge pushing back (both contain a frictional component). If the force was from an adjacent wedge, then the reaction force was used as input into the next wedge. This process was used until the last wedge was reached for

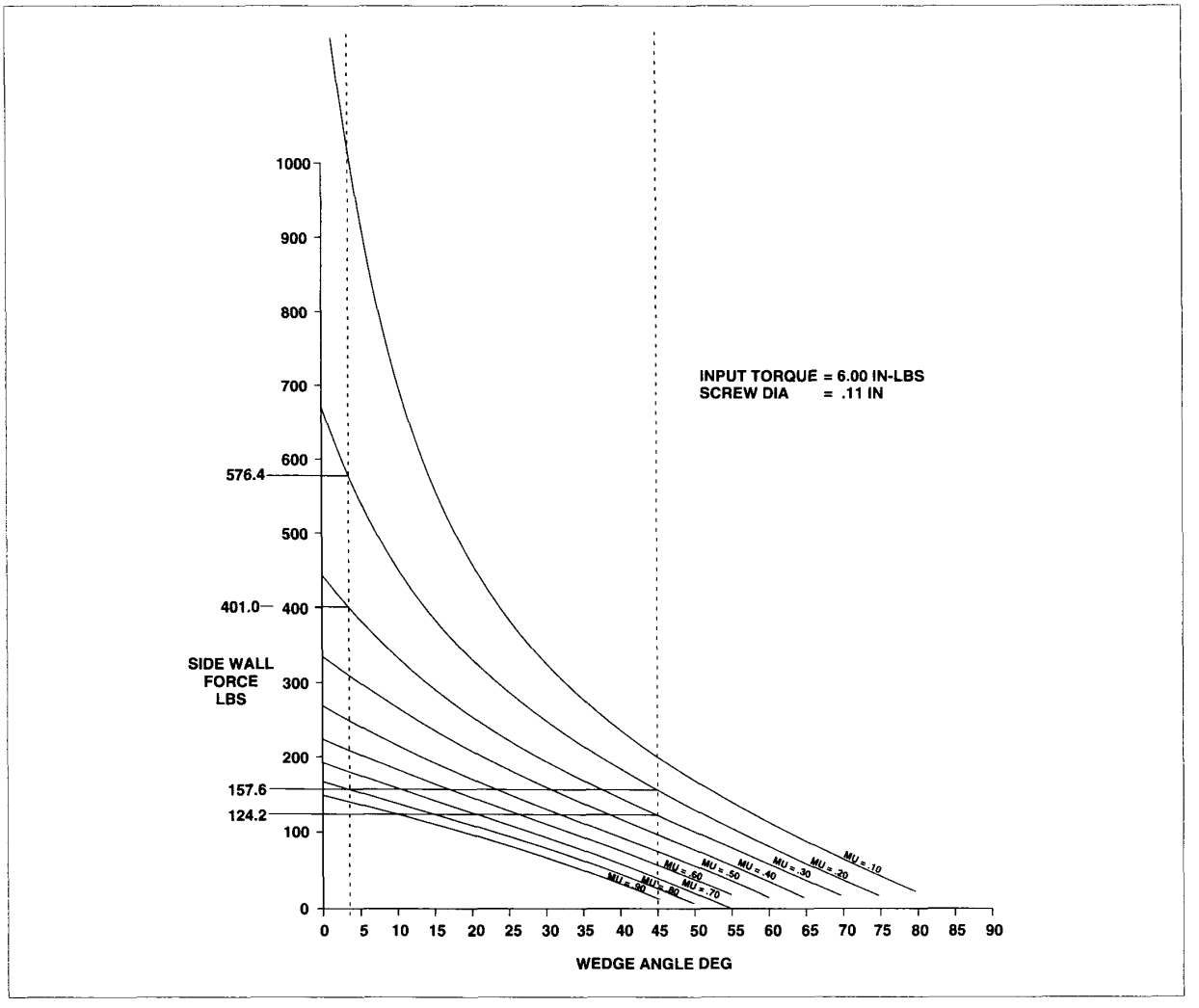

Figure 5. Wedge Angle Versus Side Wall Force

the end-fixed condition, or the center wedge was reached for the center-fixed condition.

$$\Theta = \text{ARCTAN}(\mu) \qquad (1)$$

where

(μ) = coefficient of friction
W = applied load
R = resultant force
N = normal force

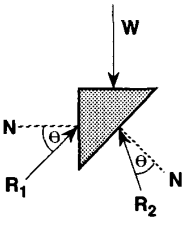

This force distribution is used as input into the finite difference computer model.

Contact Area and Pressure

Once the internal forces (wedge to wedge) and external forces (wedge and thermal core to chassis) have been determined, the contact area for each mating interface must be determined. Using the physical wedge dimensions will only provide a calculated maximum contact area that is very different from the area determined empirically under loaded conditions. If the actual area is not used, then the resultant pressure calculations will be incorrect, as will also the final estimated thermal resistance.

When the card clamps are torqued down, the clamp and thermal core undergo minute deflections. These deflections result in an uneven distribution of the loading across the card interface and thereby create a reduced contact area. To obtain an accurate value for the contact area, a pressure sensitive two-part film from FUJI® film was used*; the film provides a permanent record of the macroscopic interface area under loaded conditions, which values are used for pressure and thermal resistance calculations.

*The film contains microencapsulated dye filled beads which burst under a predetermined pressure and release their dye. This dye in turn bleeds into the adjacent part which contains the developer.

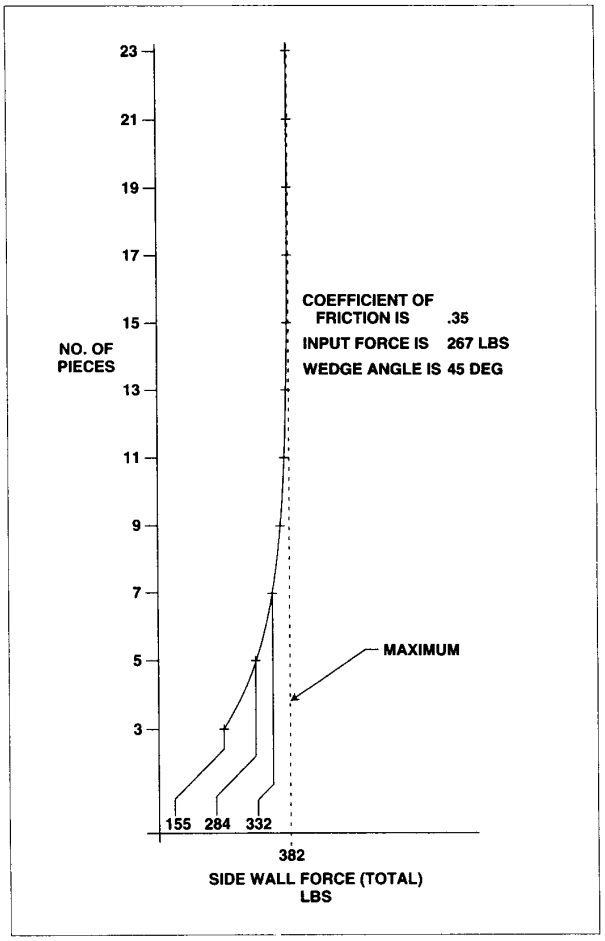

Figure 6. Side Wall Force Versus Number of Wedges

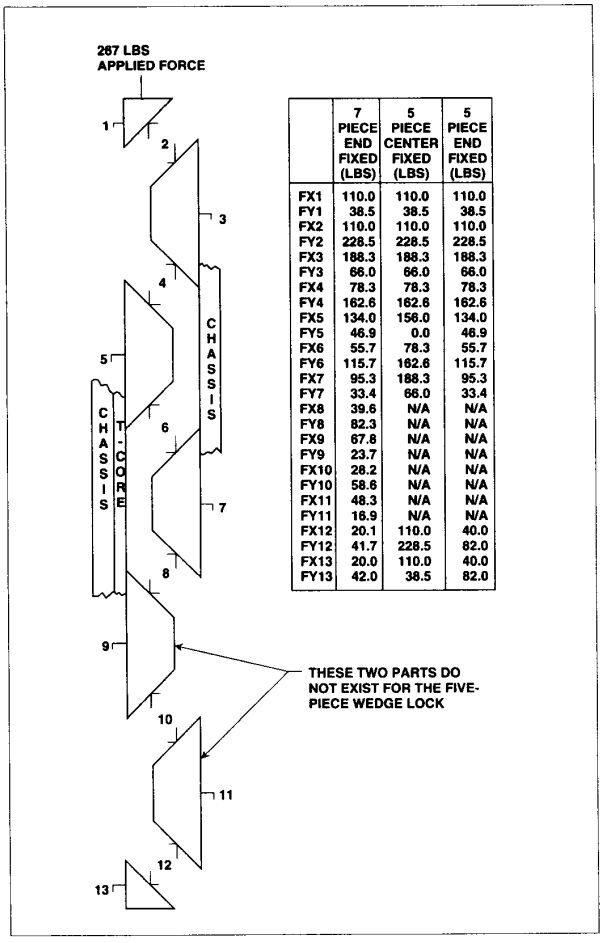

	7 PIECE END FIXED (LBS)	5 PIECE CENTER FIXED (LBS)	5 PIECE END FIXED (LBS)
FX1	110.0	110.0	110.0
FY1	38.5	38.5	38.5
FX2	110.0	110.0	110.0
FY2	228.5	228.5	228.5
FX3	188.3	188.3	188.3
FY3	66.0	66.0	66.0
FX4	78.3	78.3	78.3
FY4	162.6	162.6	162.6
FX5	134.0	156.0	134.0
FY5	46.9	0.0	46.9
FX6	55.7	78.3	55.7
FY6	115.7	162.6	115.7
FX7	95.3	188.3	95.3
FY7	33.4	66.0	33.4
FX8	39.6	N/A	N/A
FY8	82.3	N/A	N/A
FX9	67.8	N/A	N/A
FY9	23.7	N/A	N/A
FX10	28.2	N/A	N/A
FY10	58.6	N/A	N/A
FX11	48.3	N/A	N/A
FY11	16.9	N/A	N/A
FX12	20.1	110.0	40.0
FY12	41.7	228.5	82.0
FX13	20.0	110.0	40.0
FY13	42.0	38.5	82.0

Figure 7. Free Body Diagram for a Typical Wedge Clamp

Figure 8 shows values for both the theoretical maximum area and the measured area of surface contact for both the card clamp to chassis interface and the thermal frame to chassis interface. The percentage of area in contact at a pressure above 350 psi is quite low, ranging from 20-37 percent. While this method was not practical for the actual contact area between wedges, a satisfactory assumption is to use the theoretical maximum area because the pressure at this interface is an order of magnitude greater than any other interface, and interface contact is considered to be 100 percent.

Modeling the Thermal Resistance

Eq.(2)[2] is used to calculate the wedge surface contact portion (or solid portion of Figure 2) of the resistance across the interface in °C/watt.

$$R_s = 0.80 \frac{\sigma}{AK_s m} \left(\frac{P}{H}\right)^{-0.95} \quad (2)$$

where R_s = contact resistance (°C/watt)

$\sigma = (\sigma_1^2+\sigma_2^2)^{0.5}$ combined RMS roughness (in.)*

*Subscript 1 and 2 denote materials 1 and 2 e.g., core material and chassis material.

A = interface contact area (in^2)

$k_s = 2*(k_1+k_2)/(k_1+k_2)$ harmonic mean thermal conductivity (W/in°C)

$m = (m_1^2+m_2^2)^{0.5}$ absolute average asperity slope (radians)

P = pressure at the interface (psi).

H = microhardness of the softer material (psi).

The resistance of the interstitial fluid (usually air) which resides between mating surfaces, in microscopic cavities (Figure 2), can be approximated using eqs.(3 and 4)[2].

$$R_g = \frac{Y+M\sigma}{AK_g} \quad (3)$$

where R_g = fluid contact resistance (°C/watt)

Y = separation distance between the mean planes of the contacting rough surfaces (in.)

M = a complex function of the thermophysical properties of the interstitial gas in combination with the materi als at the interface (for air at 1 atmosphere and 100°C, M = 0.80).

k_g = Thermal conductivity of the interstitial fluid in the gap (W/in°C)

$$Y = 1.53\sigma\left(\frac{P}{H}\right)^{-0.97} \quad (4)$$

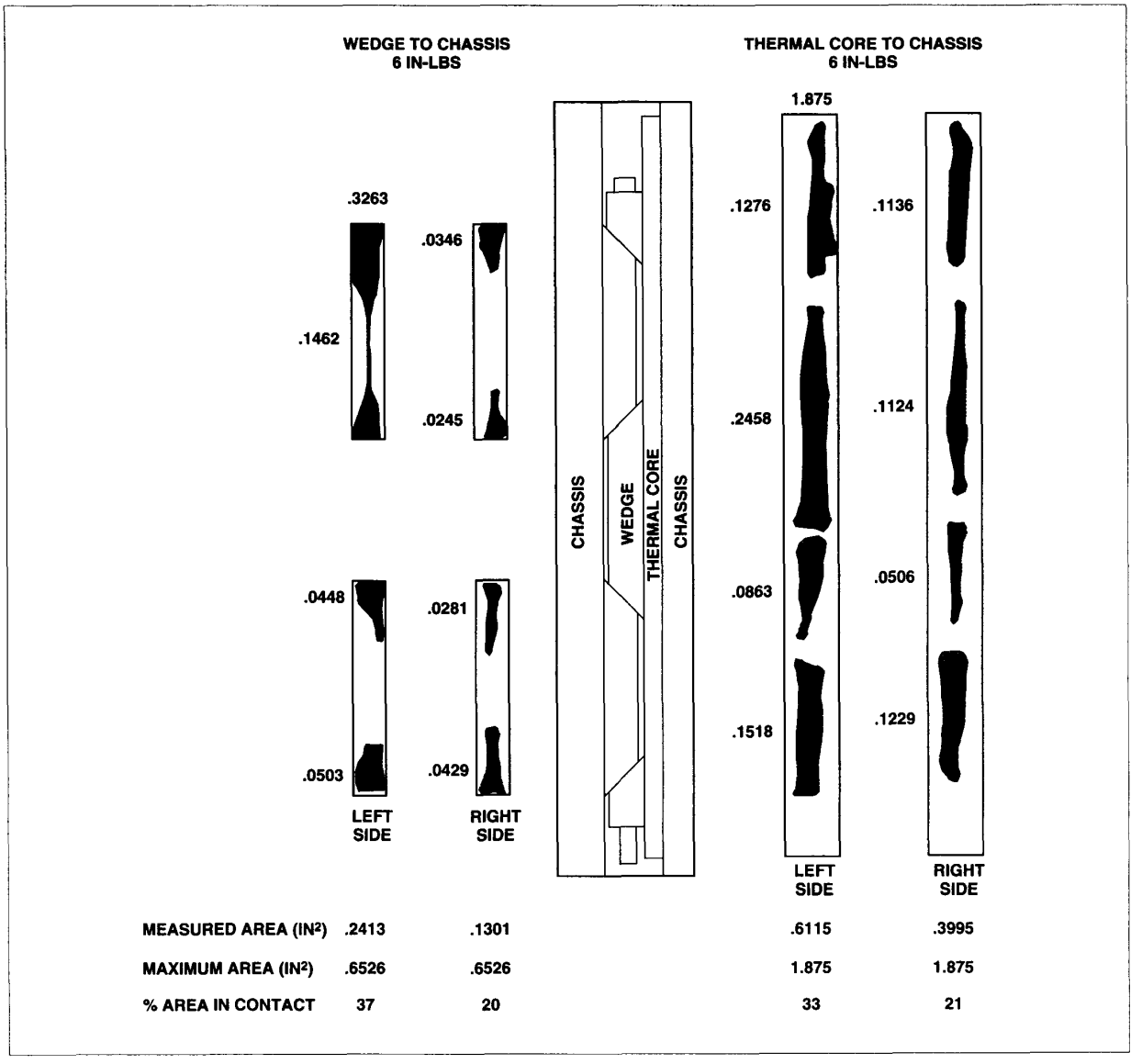

Figure 8. Measured Contact Area for Five-piece Clamp

When using relatively soft materials (such as 6061-T6 aluminum) at the interface, the value for the resistance due to the interstitial fluid is approximately 100 times that for the solid portion of the contact resistance. When placed in parallel with the solid resistance, the air gap resistance has very little effect and therefore has been purposefully left out of the model. This assumption should not be made when using very hard or smooth materials, such as hardened steels and ceramics.

The finite difference model shown in Figure 9 is used to determine the total interface resistance (only half of the model is shown due to the symmetry in a center-fixed wedge clamp). The model is constructed using the following guidelines. The force distribution and the contact area are placed into the resistance equation (Eq. 2) to determine the resistance for each mating surface (output of the Unigraphics® GRIP® routine). This resistance is then converted into a conductance value (1/R) and distributed between the nodes of the particular surface as conductors in parallel. This step is repeated for each pair of mating surfaces. The material conductances are added for the remaining elements, input power is evenly distributed along the center row of nodes of the thermal core, and the chassis wall on both sides is set to zero to determine the final overall temperature rise at each chassis to CCA interface.

Appendix A contains an example of the output from the Unigraphics® GRIP® routine which determines the interface resistances, and measured temperatures for a VME-sized core. The output and temperature data are for a design utilizing a five-piece center-fixed wedge clamp with an applied load of 150 lbs at 50, 100, and 150 watts.

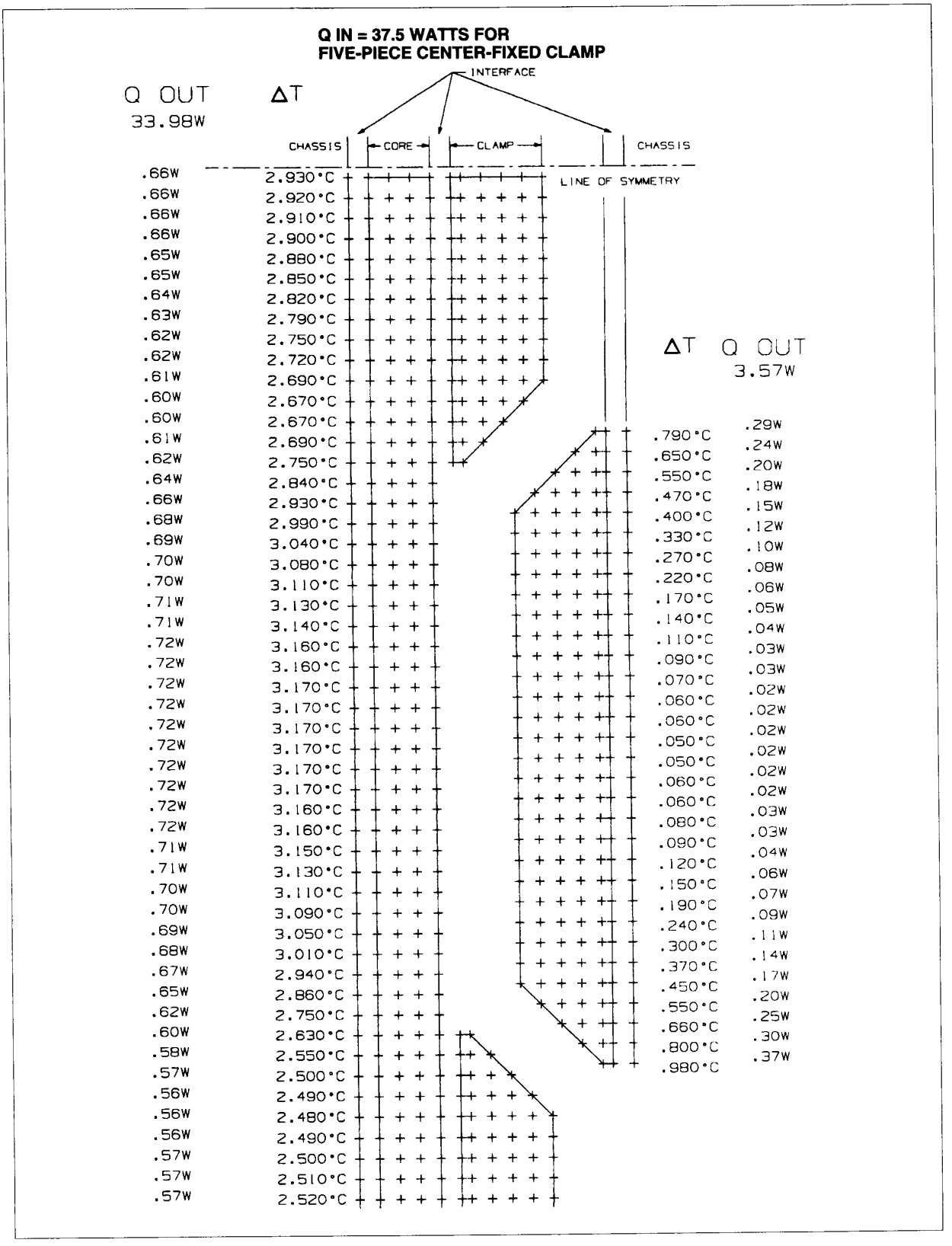

Figure 9. Finite Difference Model

Conclusions

Modeling the interface included a number of variables. This paper provides a methodology for determining the interface resistance and relies heavily on previously documented experimental and theoretical values for many of the parameters.[2, 3, 4] Modification of any of these design parameters may greatly affect the calculated thermal resistance value. The important factors incorporated in this model are the use of distributed load force values along the length of the interface (which may vary greatly depending on the type of clamp used) and using the actual contact area versus apparent or calculated area. One resistance that is not included in the example but has a significant effect on the interface resistance is that of corrosion protective finishes. Values associated with material finishes must be determined and added to get the net interface resistance. For example, a type III hard anodize finish changes the surface finish characteristics (it can increase the interface resistance up to 0.36 °C/W for SEM-E[1]) and therefore would require a new analysis run. A chemical film coating such as iridite does not appreciably change the surface finish and would only require adding the resistance of the film in series with the base metal.

Although our preliminary testing has led to values of approximately 0.15°C/W (5.5°C rise with 37.5-watt input power), the values of interface resistance in the order of 0.50 °C/W have been reported[1] which result in a temperature rise of 19°C for a 75-watt SEM-E CCA. It is therefore increasingly important to reduce, or develop designs to eliminate, the contribution of this interface to the overall temperature rise of a CCA. When determining which chassis interface to emphasize, Figure 9 shows that approximately 90 percent of the heat load exits through the thermal core to chassis interface and only 10 percent exits through the wedge clamp to chassis interface. This leads to an emphasis on clamp designs that provide adequate and uniform pressure distribution at the thermal core to chassis interface, and on core/chassis designs that improve the contact area at this interface.

Areas for further research to improve heat transfer and reduce the error within the analysis include modifying clamp designs to provide increased contact area (i.e., pre-bending wedge segments), developing protective finishes with improved heat transfer characteristics (i.e., diamond film), creating standard formats that eliminate the interface, acquiring improved experimental data on heat sink and wedge clamp material characteristics (i.e., values for microhardness and asperity slope), correlating more test data with eq. 2 to determine a range for the exponent (-0.95), and more closely determining coefficients of friction between wedge clamp segments.

References (Cited)

[1] D. Maass, "Trends in Conduction Cooling for Avionics," *Computer Packaging Technology*, September 1993, pp. 56-59.

[2] Vincent W. Antonetti and Jeffrey C. Eid, "Measuring Thermal Contact Resistance," *Proceedings Sixth International Electronics Packaging Conference*, San Diego, CA, November 1986.

[3] TP529, *Standard Electronic Modules Program Thermal Applications Handbook*, Naval Weapons Support Center Crane, Crane, IN, 47522.

[4] M. M. Yovanovich, "Thermal Contact Correlations," Paper 81-1164, *Technical papers from the AIAA 16th Thermophysics Conference*, Palo Alto, CA, June 23-25, 1981.

References (Not Cited)

[1] M. M. Yovanovich and A. Hegazy, "Experimental Verification of Contact Conductance Models Based Upon Distributed Surface Micro-Hardness," Paper AIAA-83-0532, *Proceedings AIAA 21st Aerospace Sciences Meeting*, Reno, NV, January 10-13, 1983.

[2] *Joint Integrated Avionics Working Group Standard Electronic Module Retention Clamp Final Test Report,* 29 April 1992, Systems Design and Analysis, Inc., Indianapolis, IN.

[3] L. S. Fletcher, M. A. Lambert, E. E. Marotta, and J. D. Adams, "Thermal Enhancement Techniques for SEM Guide Ribs and Card Rails."

[4] B. R. Simon, A. Ortega, M. Kaufmann, K. Hnat, Y. Yuan, Y. Cui, and J. L. Prince, "Finite Element and Experimental Procedures for Determining Thermal Contact Resistance," *Proceedings ASME Winter Annual Meeting,* November 8-13, Anaheim, CA.

[5] M. M. Yovanovich, "Thermal Contact Resistance in Microelectronics."

[6] C. V. Madhusudana and L. S. Fletcher, "Gas Conductance Contribution to Contact Heat Transfer," Paper 81-1163, *Technical Papers from the AIAA 16th Thermophysics Conference*, Palo Alto, CA, June 23-25, 1981.

Appendix A

Example of the output of the Unigraphics® GRIP® routine.

```
SUM OF FORCES LEFT SIDE : 204.806
SUM OF FORCES RGHT SIDE : 204.806
RETENTION FORCE         : 184.325


FX1 : 59.9411 X
FY1 : 26.9735 Y

FX2 : 59.9411 X
FY2 : 158.0265 Y

FX3 : 102.4030 X
FY3 : 46.0814 Y

FX4 : 42.4620 X
FY4 : 111.9451 Y

FX5 : 84.9239 X
FY5 : .0000 Y

FX6 : 42.4620 X
FY6 : 111.9451 Y

FX7 : 102.4030 X
FY7 : 46.0814 Y

FX8 : 59.9411 X
FY8 : 158.0265 Y

FX9 : 59.9411 X
FY9 : 26.9735 Y
```

```
WEDGE ANGLE       : 45.00000 °
FRICTION ANGLE    : 24.22775 °
TOTAL ANGLE       : 69.22775 °
APPLIED LOAD      : 185.0000 lbs.
COE OF FRICTION   : .45000
K1                : 4.31800 W/in°C
K2                : 4.31800 W/in°C
WALL/WEDGE RES.   : .06173 °C/W
WEDGE/WEDGE RES.  : .07672 °C/W
WEDGE/CARD RES.   : .05785 °C/W
CLAMP MAT. RES.   : 9.09766 °C/W
CARD/WALL RES.    : .06219 °C/W
RES. THRU CLAMP   : 9.29397 °C/W
OVERALL RES.      : .06178 °C/W
SURFACE FIN 1     : 85 uin
SURFACE FIN 2     : 85 uin
ASPERITY SL 1     : .30843 RAD
ASPERITY SL 2     : .30843 RAD
MICRO HRDNSS 1    : 170322.2 PSI
MICRO HRDNSS 2    : 170322.2 PSI
TOTAL SIDE FORCE  : 204.8061 LBS
NO. OF PIECES     : 5
 K VALUE AT WALL  : .15462
```

```
TOTAL    RESISTANCE 1 IS .22565
CONTACT  RESISTANCE 1 IS .22960
GAS      RESISTANCE 1 IS 13.10544
K VALUE FOR SINDA INPUT FOR FACE 1 IS .43553
NUMBER OF NODES AT INTERFACE 10

TOTAL    RESISTANCE 2 IS .26408
CONTACT  RESISTANCE 2 IS .26446
GAS      RESISTANCE 2 IS 181.4883
K VALUE FOR SINDA INPUT FOR FACE 2 IS .75626
NUMBER OF NODES AT INTERFACE 5

TOTAL    RESISTANCE 3 IS .11570
CONTACT  RESISTANCE 3 IS .12400
GAS      RESISTANCE 3 IS 1.72824
K VALUE FOR SINDA INPUT FOR FACE 3 IS .25201
NUMBER OF NODES AT INTERFACE 32

TOTAL    RESISTANCE 4 IS .36622
CONTACT  RESISTANCE 4 IS .36694
GAS      RESISTANCE 4 IS 185.7840
K VALUE FOR SINDA INPUT FOR FACE 4 IS .54504
NUMBER OF NODES AT INTERFACE 5

TOTAL    RESISTANCE 5 IS .13833
CONTACT  RESISTANCE 5 IS .14801
GAS      RESISTANCE 5 IS 1.72696
K VALUE FOR SINDA INPUT FOR FACE 5 IS .22520
NUMBER OF NODES AT INTERFACE 30

TOTAL    RESISTANCE 6 IS .36622
CONTACT  RESISTANCE 6 IS .36694
GAS      RESISTANCE 6 IS 185.7840
K VALUE FOR SINDA INPUT FOR FACE 6 IS .54504
NUMBER OF NODES AT INTERFACE 5

TOTAL    RESISTANCE 7 IS .11570
CONTACT  RESISTANCE 7 IS .12400
GAS      RESISTANCE 7 IS 1.72824
K VALUE FOR SINDA INPUT FOR FACE 7 IS .25201
NUMBER OF NODES AT INTERFACE 32

TOTAL    RESISTANCE 8 IS .26408
CONTACT  RESISTANCE 8 IS .26446
GAS      RESISTANCE 8 IS 181.4883
K VALUE FOR SINDA INPUT FOR FACE 8 IS .75626
NUMBER OF NODES AT INTERFACE 5

TOTAL    RESISTANCE 9 IS .22565
CONTACT  RESISTANCE 9 IS .22960
GAS      RESISTANCE 9 IS 13.10544
K VALUE FOR SINDA INPUT FOR FACE 9 IS .43553
NUMBER OF NODES AT INTERFACE 10
```

Example of measured temperature data and a figure of the test set-up.